Development of mouse models of angiosarcoma driven by p53

First posted online on 20 June 2019 as 10.1242/dmm.038612
Access the most recent version at http://dmm.biologists.org/lookup/doi/10.1242/dmm.038612

Development of mouse models of angiosarcoma driven by p53

Donald M Salter[1], Meredyth Griffin[2], Morwenna Muir[2], Katy Teo[2], Jayne Culley[2], James R Smith[3], Laura Gomez-Cuadrado[2], Kylie Matchett[3], Andrew H Sims[2], Larry Hayward[2], Neil C Henderson[3], Valerie G Brunton[2*]

[1]Centre for Genomic & Experimental Medicine, Institute of Genetics & Molecular Medicine, University of Edinburgh, Crewe Road South, Edinburgh, EH4 2XR

[2]Edinburgh Cancer Research UK Centre, Institute of Genetics & Molecular Medicine, University of Edinburgh, Crewe Road South, Edinburgh, EH4 2XR

[3]Centre for Inflammation Research, The Queen's Medical Research Institute, University of Edinburgh, Little France Crescent, Edinburgh, EH16 4TJ

*Corresponding author: Prof Valerie Brunton
v.brunton@ed.ac.uk

Conflict of Interest Statement: the authors have no conflict of interest to declare

Abstract

Angiosarcomas are a rare group of tumours which have poor prognosis and limited treatment options. The development of new therapies has been hampered by a lack of good preclinical models. Here we describe the development of an autochthonous mouse model of angiosarcoma driven by loss of p53 in VE-cadherin expressing endothelial cells. Using *Cdh5-Cre* to drive recombination in adult endothelial cells, mice developed angiosarcomas with 100% penetrance upon homozygous deletion of *Trp53* with a median lifespan of 325 days. In contrast, expression of the R172H mutant p53 resulted in formation of thymic lymphomas with a more rapid onset (median lifespan 151 days). We also used *Pdgfrb-Cre* expressing mice which targets predominantly pericytes, as these have been reported as the cell of origin for a number of soft tissue sarcomas. *Pdgfrb-Cre* also results in low levels of recombination in venous blood endothelial cells in multiple tissues during development. Upon deletion of *Trp53* in *Pdgfrb*-Cre, $Trp53^{fl/fl}$ mice 65% developed lymphomas and 21% developed pleomorphic undifferentiated soft tissue sarcomas. None developed angiosarcomas. In contrast, 75% of *Pdgfrb*-Cre, $Trp53^{R172H/R172H}$ mice developed angiosarcomas with 60% of these mice also developing lymphomas. The median lifespan of the *Pdgfrb*-Cre, $Trp53^{R172H/R172H}$ mice was 151 days. Re-implantation of angiosarcoma tumour fragments from *Cdh5-Cre*, $Trp53^{fl/fl}$ mice provided a more consistent and rapid model of angiosarcoma than the two spontaneous models. The ability to passage tumour fragments through the mouse provides a novel model which is amenable to preclinical studies and will help the development of potential new therapies for angiosarcoma.

Key Words: angiosarcoma, p53, genetically engineered mouse model

Introduction

Angiosarcomas are rare but aggressive endothelial cell tumours. Most arise spontaneously but they also develop following ionizing radiation and chronic lymphedema. They have a high risk of local recurrence and metastasis with limited treatment options such that the overall 5-year survival is around 35% [1]. They typically express endothelial markers such as CD31 and vascular endothelial growth factor (VEGF) and for this reason there is interest in the use of anti-angiogenic therapies for their treatment. Data from a number of clinical trials show promising activity of the VEGF-A monoclonal antibody bevacizumab and broad spectrum, small molecule tyrosine kinase inhibitors that target VEGF receptors [1]. However, the underlying pathways driving the pathogenesis of angiosarcoma are not well defined and together with the urgent need for effective therapies we set out to develop an autochthonous mouse model of angiosarcoma that could aid preclinical drug development efforts.

Mutations in *TP53* have been reported in human angiosarcomas with incidences of between 4 and 52% reported in different studies [2-8]. In addition, mice with germline deletion of *Trp53* which are pre-disposed to development of lymphoma develop angiosarcomas in significant numbers [9,10]. The predominance and rapid development of lymphoma in these models precludes their usefulness as models of angiosarcoma. Attempts have therefore been made to overcome this by use of tissue specific Cre-Lox recombination of conditional alleles and alymphocytic mice [11,12].

There is increasing evidence that mesenchymal stem cells (MSCs) may be the cell of origin of a number of different sarcoma sub-types [13-18]. Coupled with the evidence that pericytes have been proposed as the identity of MSCs in normal tissues [19,20] and some sarcomas share

features of pericytes such as expression of NG2 and CD146 [21,22], we set out to address whether *Pdgfrb*-Cre and *Cdh5-CreER*^{T2} mice could be utilized to generate a model of angiosarcoma. *Pdgfrb*-Cre mice express Cre recombinase under the control of a fragment of the gene encoding platelet-derived growth factor receptor-β (PDGFR-β). This drives Cre mediated recombination in pericytes in a number of tissues [23,24] and low levels of recombination in venous blood endothelial cells in multiple tissues during development [25,26]. This allows us to target loss of p53 function to the pericyte lineage while also potentially targeting endothelial cell lineages. *Cdh5-CreER*^{T2} mice express Cre recombinase under the inducible control of the vascular endothelial cadherin (VE-cadherin; *Cdh5*) promoter in adult mice to drive expression in endothelial cells [27].

It is widely accepted that mutant forms of p53 can exert dominant negative or gain-of-function effects that contribute to tumour development beyond that seen following loss of the wild type p53 protein alone [28,29]. Individuals with Li-Fraumeni syndrome carry inherited mutations in *TP53* and are predisposed to tumour development including sarcomas. In mouse models of Li-Fraumeni syndrome expression of *Trp53R172H*, which corresponds to the *TP53R175H* hot spot mutation in human tumours, mice develop predominantly lymphomas but a small percentage also develop angiosarcomas [30,31]. We therefore generated mice in which *Trp53R172H* was expressed under the control of *Pdgfrb-Cre* and *Cdh5-CreER*^{T2} in addition to those carrying a floxed *Trp53* allele.

Materials and Methods

Animals

Mice expressing *Cre* under the control of the *Pdgfrb* promoter (*Pdgfrb-Cre*) [23] or in the inducible control of the *Cdh5* promotor (*Cdh5-CreER*^{T2}) [27], were crossed to mice expressing either a mutant p53R172H [31] or floxed p53 allele [32] to give experimental cohorts on a mixed background segregating for C57BL/6J and S129 genomes. The mutant p53 allele is preceded by a STOP cassette, flanked by LoxP sites, such that upon activation of Cre recombinase the STOP cassette is excised and the mutant p53R172H expressed, while in the floxed p53 mice activation of Cre deletes exons 2-10 resulting in a loss of p53. *Pdgfrb-Cre* and *Cdh5-CreER*^{T2} mice were also crossed with Ai14 (Rosa-CAG-LSL-tdTomato-WPRE) mice [33], obtained from the Jackson Laboratory, to allow endogenous reporting in *Pdgfrb and Cdh5* expressing cells. Genotyping was carried out by Transnetyx (Cordova, TN). *Cdh5-CreER*^{T2} mice were treated with tamoxifen (Sigma) (100 mg/kg, i.p.) for 5 days at 6 weeks of age. Mice were monitored twice weekly and sacrificed when cutaneous tumours had reached a maximum size of 1.5 cm or became sickly as defined by UK Home Office guidelines. Following sacrifice macroscopically identified tumours and major organs were removed and fixed in 10% neutral buffered formalin. In some instances, fresh samples were taken for generation of cell lines or tumour fragments taken for re-implantation. Animal studies and procedures were approved by the University of Edinburgh Ethical review committee (Application #PL01-16) and conducted in accordance with United Kingdom Home Office regulations.

Histology and immunohistochemistry

Formalin fixed tissues were routinely processed into paraffin wax blocks and sections cut for H&E staining and immunohistochemistry. Immunohistochemistry was carried out as previously described [34]. Primary antibodies used were CD31 at 1:800 (Abcam, ab28364), ERG (Dako, IR659), p53 at 1:2000 (Leica BioSystems, NCL-L-p53-CM5p), PDGFRβ at 1:100 (CST, 3169S), and VE-cadherin at 1:4000 (Abcam, ab33168).

Immunofluorescence

Shaved dorsal skin was mounted on 3 mm blotting paper and placed in 4% methanol-free formaldehyde (Thermo-Fisher Scientific, 28906) at 4°C for one hour. The skin was then washed with PBS and transferred to 18% sucrose overnight for cryoprotection prior to embedding in OCT embedding matrix (Cellpath, KMA-0100-00A) and frozen on dry ice. 7 μm cryotome sections were dried at room temperature in the dark for 30 minutes and washed in PBS containing 0.05% Tween 20 (Sigma Aldrich, P2287). To image endogenous tdTomato fluorescence, sections were incubated with 1 μM DAPI for 10 minutes, washed twice with PBS, and mounted with Prolong Gold (Thermo-Fisher Scientific, P36930). For indirect immunofluorescence staining, sections were incubated with blocking buffer (PBS containing 5% goat serum (Vector, S-1000) and 0.3% Triton X100 (Sigma Aldrich, T8787) for 30 minutes, then incubated with primary antibodies PDGFRβ (1:25, Abcam Ab32570) or CD31 (1:50, BD Pharmingen 550274) for 2 hours. Sections were then washed twice and incubated for 30 minutes with Alexafluor 488 conjugated secondary antibodies (Molecular Probes Inc - goat anti-rabbit 488 (A11034) or goat anti-rat 488 (A11006), washed twice, incubated with DAPI and mounted as described above. Images were obtained on a Zeiss LSM780 confocal microscope.

Cell culture

Tumours from *Pdgfrb*-Cre, *p53*$^{R172H/R172H}$ mice were freshly processed by rinsing in PBS and then mincing to ~1 mm^3 pieces using two scalpels. After transferring to a 15 ml Falcon tube containing 10 mL digestion media (maintenance medium omitting fetal bovine serum (FBS) and including 300 U/mL collagenase I (Worthington) and 100 U/mL hyaluronidase (Fisher), cells were subjected to shaking incubation at 37°C for 18 hours. After pelleting at 1300 rpm for 5 minutes cells were resuspended in 2 mL maintenance media (DMEM/Ham's F12 (Sigma), 10% FBS (Gibco), amphotericin (Gibco) and penicillin-streptomycin (Sigma)) before being transferred to a six well plate. Cells were left undisturbed for 5-7 days in a humidified incubator at 37°C with 5% CO_2 before refreshing media and moving on to flasks when confluent. Tumours from *Cdh5-CreER*^{T2}, *Trp53*$^{fl/fl}$ mice were manually minced using scalpels and left undisturbed for 5-7 days before transferring to flasks when confluent. Cells were maintained in Ham's F-12K Medium (Gibco), 10% FBS (Gibco), amphotericin B (Gibco), penicillin-streptomycin (Sigma), 0.1 mg/mL heparin (Sigma) plus 20 µg/mL endothelial cell growth supplement (Sigma, E2759) and checked routinely for mycoplasma infection.

Western analysis

SDS denatured protein samples made from RIPA lysates were run on 4-15% precast polyacrylamide gels (Biorad) in Tris/Glycine/SDS running buffer (Biorad) and transferred onto nitrocellulose using the Trans-Blot® Turbo System (Biorad). After blocking the membrane in 5% BSA in PBS, anti-p53 antibody (VectorLabs, VP-P955) was added at 1:50 overnight at 4°C on a shaking platform. The membrane was washed in TBS-T thrice before being incubated with an HRP conjugated anti-rabbit secondary antibody (CST, #7074) at 1:1000). Washes were repeated and then the membrane visualized on a ChemiDoc (BioRad) using ECL western blotting substrate (Pierce).

Gene expression profiling

RNA prepared from angiosarcomas that developed in the *Pdgfrb*-Cre, $p53^{R172H/R172H}$ and *Cdh5-CreER*^{T2}, $Trp53^{fl/fl}$ mice was analyzed using the NanoString PanCancer Pathways panel (represents 750 cancer associated genes) on the NanoString nCounter DX platform as per the manufacturer's instructions. For comparison Cdh5 positive liver endothelial cells were isolated from Ai14;*Cdh5-CreER*^{T2} mice 3 weeks following tamoxifen treatment [35]. A Cdh5 (tdTomato) positive population of endothelial cells was collected using a BD FACSAria II. Following standard nCounter normalisation differentially expressed genes were identified using Student's t-tests ($p<0.05$) between the angiosarcomas derived from the *Pdgfrb*-Cre, $p53^{R172H/R172H}$ and *Cdh5-CreER*^{T2}, $Trp53^{fl/fl}$ mice and relative to the normal endothelial cells. Hierarchical cluster analysis was performed with the Cluster and Treeview programs [36]. Gene set enrichment analysis [37] was performed using the Phenotest R package. Gene ontology analysis was performed using the PANTHER classification system [38].

Sub-cutaneous tumour growth

Cell lines and tumour fragments derived from the mouse angiosarcomas were injected into both flanks of 6-8 week old female CD-1 nude mice (Charles River) and tumour growth measured twice weekly using calipers. Tumour volumes were calculated in Excel using the formula $v = 4/3\pi r^3$. Animals were sacrificed when tumours reached the maximum size allowed and collected and fixed in 10% neutral buffered formalin.

RESULTS

Tumour development in *Pdgfrb*-Cre, *Trp53*$^{R172H/R172H}$ and *Pdgfrb*-Cre, *Trp53*$^{fl/fl}$ mice

Experimental cohorts consisted of mice expressing either one (*Pdgfrb-Cre, Trp53*$^{R172H/+}$) (n=16) or two (*Pdgfrb-Cre, Trp53*$^{R172H/R172H}$) (n=28) mutant *Trp53*^{R172H} alleles or loss of both *Trp53* alleles (*Pdgfrb*-Cre, *Trp53*$^{fl/fl}$) (n=14). The median lifespan of the *Pdgfrb-Cre, Trp53*$^{R172H/R172H}$ mice was 93 days compared to >365 days for the *Pdgfrb-Cre, Trp53*$^{R172H/+}$ mice and 189.5 days for the *Pdgfrb*-Cre, *Trp53*$^{fl/fl}$ mice (Figure 1A). The deaths of all *Pdgfrb-Cre, Trp53*$^{R172H/R172H}$ mice were due to tumour formation in contrast to the *Pdgfrb-Cre, Trp53*$^{R172H/+}$ cohort where only 2/16 mice were culled due to tumour formation. In the *Pdgfrb*-Cre, *Trp53*$^{fl/fl}$ cohort 12/14 mice were culled due to tumour formation. Mice that were asymptomatic at 1 year of age were culled.

Autopsy findings and tumour histology

In the *Pdgfrb-Cre, Trp53*$^{R172H/R172H}$ cohort 75% (n=21/28) of the mice developed angiosarcomas. Of these 21 mice, 9 demonstrated only angiosarcomas whilst in the other 12 mice lymphomas were also identified. The remaining *Pdgfrb-Cre, Trp53*$^{R172H/R172H}$ mice developed either lymphomas (n=5/28) or teratomas (n=2/28) (Figure 1B). Thus, the predominant tumour type was angiosarcoma with most mice developing multiple angiosarcomas in a number of different organs (Table 1) (Figure 1B: median 3, range 1-6 tumours). No angiosarcomas were seen in the *Pdgfrb-Cre, Trp53*$^{R172H/+}$ mice. The 2 *Pdgfrb-Cre, Trp53*$^{R172H/+}$ mice culled due to tumour formation had developed lymphomas. At autopsy, following culling of the asymptomatic *Pdgfrb-Cre, Trp53*$^{R172H/+}$ mice at 1 year, 3 were found

to have developed lymphomas and 1 adenocarcinoma in the lung. The remainder showed no gross or histological abnormality (Figure 1C). Within the *Pdgfrb*-Cre, *Trp53*$^{fl/fl}$ mice 9 developed lymphomas and 3 undifferentiated sarcomas upon histological examination, while the remaining 2 had no detectable tumour upon sacrifice (Figure 1D).

Characterization of angiosarcomas in *Pdgfrb*-Cre, *Trp53*$^{R172H/R172H}$ mice

The morphological appearances of the angiosarcomas were similar within and between mice. The tumours consisted of lobules of pleomorphic cells showing varying degrees of vascular formation typical of high-grade angiosarcomas (Figure 2A, B). Immunohistochemistry supported the morphological assessment with the tumour cells expressing CD31 and ERG (Figure 2C, D). There was no expression of CD34 by the tumour cells (not shown). The tumours also showed strong expression of p53 (Figure 2E) in keeping with the stabilization of mutant p53 that is often seen in human tumours expressing mutant p53. PDGFR-β was expressed by stromal cells within the tumour masses but not reliably by the angiosarcomatous cells (Figure 2F).

Development of undifferentiated sarcomas in *Pdgfrb*-Cre, *Trp53*$^{fl/fl}$ mice

Three of the 14 (21%) *Pdgfrb*-Cre, *Trp53*$^{fl/fl}$ mice developed tumours with the morphological features of high-grade spindle cell and pleomorphic undifferentiated soft tissue sarcoma (Figure S1A). Immunohistochemistry showed no expression of p53 confirming the homozygous deletion of p53 in the *Pdgfrb*-Cre, *Trp53*$^{fl/fl}$ mice (Figure S1B) and strong expression of PDGFR-β by the tumour cells (Figure S1C). Less than 10% of the cells expressed SMA in 2 of the cases whilst the other was completely negative for SMA. None of the tumour cells expressed CD31 (Figure S1D) or ERG (not shown).

PDGFR-β Cre recombination does not occur in adult CD31 endothelial cells

As the angiosarcomas that developed expressed CD31 but did not express PDGFR-β we asked whether there was any Cre mediated recombination in CD31 positive endothelial cells in adult mice. Using Ai14 reporter mice (single-fluorescent reporter mice that express tdTomato after Cre-mediated recombination)[33] we found that *Pdgfrb-Cre* induced highly efficient recombination in mouse skin (Figure 3A), a tissue where a number of angiosarcomas arose in the *Pdgfrb-Cre, Trp53*$^{R172H/R172H}$ mice. To evaluate the specificity of recombination, we stained skin from Ai14;*Pdgfrb-Cre* mice for PDGFR-β and confirmed appropriate reporter expression by *Pdgfrb-Cre* (Figure 3B). Staining of Ai14;*Pdgfrb-Cre* mice skin for CD31 expression showed that recombination did not target adult endothelial cells and in some cases PDGFR-β expressing cells were seen surrounding small CD31 positive endothelial cells (Figure 3C). This suggests that the angiosarcomas have arisen either from endothelial cell lineages that transiently express PDGFR-β during development [25,26] or from other PDGFR-β expressing pericyte lineages. Interestingly the undifferentiated sarcomas that developed in the *Pdgfrb*-Cre, *Trp53*$^{fl/fl}$ mice had retained expression of PDGFR-β suggesting a different cell of origin.

Tumour development in *Cdh5-CreER*^{T2}, *Trp53*$^{R172H/R172H}$ and *Cdh5-CreER*^{T2}, *Trp53*$^{fl/fl}$ mice

To determine whether we could promote more efficient generation of angiosarcomas we directly induced expression of mutant p53 or loss of p53 in adult endothelial cells using *Cdh5-CreER*^{T2} mice where Cre recombinase is driven by *Cdh5*, which encodes the endothelial specific VE-cadherin. Using Ai14;*Cdh5-CreER*^{T2} reporter mice we found that *Cdh5-Cre* induced recombination in CD31 positive endothelial cells (Figure S2). Experimental cohorts consisted of mice expressing either one (*Cdh5-CreER*^{T2}, *Trp53*$^{R172H/+}$) (n=15) or two (*Cdh5-*

CreER^{T2}, *Trp53*$^{R172H/R172H}$) (n=8) mutant *Trp53*^{R172H} alleles or loss of one (*Cdh5-CreER*^{T2}, *Trp53*$^{fl/+}$) (n=9) or both *Trp53* alleles (*Cdh5-CreER*^{T2}, *Trp53*$^{fl/fl}$) (n=13). A control cohort of *Cdh5-CreER*^{T2} mice were also treated with tamoxifen (n=9). The median lifespan of *Cdh5-CreER*^{T2}, *Trp53*$^{R172H/R172H}$ mice was 151 days (range 109 - 198) (Figure 4A). In the *Cdh5-CreER*^{T2}, *Trp53*$^{R172H/+}$ cohort 2/16 mice developed tumours and all others were asymptomatic mice and sacrificed at 1 year (Figure 4A, B). The median lifespan of *Cdh5-CreER*^{T2}, *Trp53*$^{fl/fl}$ mice was 325 days (range 224 - 407) (Figure 4A). All were culled due to tumour formation. All *Cdh5-CreER*^{T2}, *Trp53*$^{fl/+}$ and *Cdh5-CreER*^{T2} mice were asymptomatic at 12 months of age and culled with no evidence of tumour formation upon autopsy.

Autopsy findings and tumour histology

In the *Cdh5-CreER*^{T2}, *Trp53*$^{R172H/R172H}$ cohort 7/8 mice developed thymic lymphomas, with evidence of thymic hyperplasia in the remaining mouse, but none developed angiosarcomas (Figure 4B). Two of the mice that developed lymphomas also developed additional tumours: one an undifferentiated sarcoma and the other a hepatocellular carcinoma. In addition, one of the *Cdh5-CreER*^{T2} mice showed evidence of thymic hyperplasia with all the others showing no evidence of tumour formation upon autopsy (Figure 4B). In the *Cdh5-CreER*^{T2}, *Trp53*$^{R172H/+}$ mice two developed tumours: one a thymic lymphoma and the other an angiosarcoma (Figure 4B). At autopsy, following culling of the asymptomatic *Cdh5-CreER*^{T2}, *Trp53*$^{R172H/+}$ mice at 1 year, the remainder showed no gross or histological abnormality. Thus, the predominant tumour type driven by *Trp53*^{R172H} in the *Cdh5-CreER*^{T2} mice was lymphoma in contrast to the angiosarcomas that developed in the *Pdgfrb-Cre, Trp53*$^{R172H/R172H}$ mice. Within the *Cdh5-CreER*^{T2}, *Trp53*$^{fl/fl}$ cohort all mice developed angiosarcomas (13/13), many with multiple tumours which developed in a range of anatomical locations (Table 2) (Figure 4B). The *Cdh5-CreER*^{T2}, *Trp53*$^{fl/+}$ mice had no detectable tumour upon sacrifice. When we looked at the

latency of the angiosarcomas and the lymphomas in all experimental mice we found that the lymphomas developed more rapidly than the angiosarcomas with a median survival of 163 days (range 109 - 198) days and 325 days (range 224 - 407) respectively (Figure 4C).

Characterization of angiosarcomas in *Cdh5-CreER^{T2}, Trp53$^{fl/fl}$* mice

Many of the tumours were similar to those seen in the *Pdgfrb*-Cre, *Trp53$^{R172H/R172H}$* mice comprising lobules of pleomorphic cells showing varying degrees of vascular formation (Figure 5A). However, many of the tumours showed extensive hemorrhage and necrosis. In some tumours a cavernous / telangiectatic pattern was evident with enlarged blood-filled spaces being lined by atypical endothelial cells. Immunohistochemistry supported the morphological assessment with the tumour cells expressing ERG, CD31 and VE-cadherin but not PDGFRα (Figure 5). 12/13 tumours that developed in the *Cdh5-CreER^{T2}*, *Trp53$^{fl/fl}$* mice, did not express p53 (Figure 5F). The reason for p53 expression in the remaining angiosarcoma is not known.

Comparison of gene expression profiles of *Pdgfrb-Cre, Trp53$^{R172H/R172H}$* and *Cdh5-CreER^{T2}, Trp53$^{fl/fl}$* tumours

To understand the differences between the angiosarcomas that developed in the *Pdgfrb-Cre, Trp53$^{R172H/R172H}$* and the *Cdh5-CreER^{T2}*, *Trp53$^{fl/fl}$* mice we carried out gene expression analysis using the NanoString PanCancer Pathways panel. Tumour type specific gene expression profiles were determined by unsupervised hierarchical clustering with both tumour types also being significantly more different than normal Cdh5 derived endothelial cells (Figure 6A). Gene ontology analysis of the genes that were significantly differentially expressed between the two different angiosarcoma subsets showed that pathways linked to p53 and angiogenesis, including FGF and VEGF signalling pathways were over represented (Figure 6B). This

indicates that the gain of function *Trp53R172H* mutant drives expression of a different set of genes to those seen in the *Cdh5-CreER*^{T2}, *Trp53*$^{fl/fl}$ mice, to initiate angiosarcoma development.

To determine whether the differentially expressed genes gene changes seen in the mouse angiosarcomas reflect changes seen in human angiosarcomas we carried out gene set enrichment analysis of the differentially expressed genes in the mouse angiosarcomas compared to normal endothelial cells and compared this with published human data from a set of human angiosarcomas and normal endothelial cells (GSE4415: [39]). This showed a significant enrichment of genes associated with human angiosarcomas in the mouse tumours compared to those expressed in the normal endothelial cells (Figure 6C), indicating that the mouse angiosarcomas represent a sub-population of human angiosarcomas. Interestingly, analysis of genes associated with endothelial cell function showed that a number were significantly increased in angiosarcomas in both the human and mouse datasets (VEGFC, EPHA2), while others were differentially regulated in the human and mouse angiosarcomas (VEGF, VEGFB, KDR, MYC) (Figure 6D).

Generation of cell lines and transplantation model

We generated cell lines from 4 angiosarcomas that developed in the *Pdgfrb-Cre, Trp53*$^{R172H/R172H}$ and mice. As with the spontaneous tumours, the cell lines all expressed p53 (Figure 7A) and genotyping showed that each cell line was homozygous for the R172H allele. Upon re-implantation of the cell lines into the flanks of mice two of the lines from the *Pdgfrb-Cre, Trp53*$^{R172H/R172H}$ mice developed tumours, with morphological features of undifferentiated pleomorphic sarcomas (Figure 7Bi). Neither the generated cell lines nor the tumours retained expression of CD31 (Figure 7Bii). We also generated cell lines from four angiosarcomas that developed in the *Cdh5-CreER*^{T2}, *Trp53*$^{fl/fl}$ mice. Genotyping confirmed that each cell line was

homozygous for the floxed *Trp53* allele. However, none of the cell lines formed tumours when injected into the flanks of recipient mice. In an attempt to overcome the loss of endothelial markers upon culture of the angiosarcomas we implanted tumour fragments from three spontaneous angiosarcomas that developed in the *Cdh5-CreER*^{T2}, *Trp53*$^{fl/fl}$ mice. All formed tumours and histological examination confirmed that these were angiosarcomas expressing both CD31 and ERG (Figure 7C, D). Furthermore, secondary implantation of frozen tumour fragments resulted in successful outgrowth of angiosarcomas in recipient wild type mice (Figure 7C, D).

Discussion

We have generated two mouse models of angiosarcoma driven by deregulation of p53. We used the *Pdgfrb-Cre* mouse that is known to target both pericytes and endothelial cells during development. This resulted in 75% of *Pdgfrb-Cre*, *Trp53*$^{R172H/R172H}$ mice developing angiosarcomas, which is higher than the 62% reported when *Tie2-Cre* mice were crossed to *Trp53* floxed mice [11]. In this model p53 is deleted in both endothelium and the hematopoietic lineages. Interestingly we saw no angiosarcomas in the *Pdgfrb-Cre*, *p53*$^{fl/fl}$ mice suggesting that the *Trp53R172H* mutant is exerting a gain-of-function activity that is required for angiosarcoma development when *Pdgfrb* cells are targeted. The development of angiosarcomas in a small percentage of mice in a model of Li-Fraumeni syndrome that expresses *Trp53R172H* supports the specific involvement of mutant p53 in the development of angiosarcoma [30,31]. Analysis of *Pdgfrb-Cre* mice has shown that recombination occurs in a number of cell types during development including endothelial and mural cells [25,26] so it is not possible to define the cell of origin in the angiosarcomas that developed in the *Pdgfrb-Cre, Trp53*$^{R172H/R172H}$ mice.

The cell of origin of sarcomas remains unclear although mounting evidence suggests that they are derived from mesenchymal cells [40]. NG2/CSPG4 is a cell surface proteoglycan expressed by pericytes, which are mesenchymal cells that surround blood vessels [41]. A recent study has shown that targeting p53 loss in adult mice using NG2/CSPG4 driven Cre recombination leads to the formation of bone and soft tissue sarcomas supporting the mesenchymal origin of these tumours [17]. In this study only one angiosarcoma developed indicating that they can arise from mesenchymal precursors but that the efficiency is much lower than that of other sarcoma types such as osteosarcomas and undifferentiated pleomorphic sarcomas that were the most frequent tumour types seen. Interestingly we found that loss of p53 in the *Pdgfrb-Cre* mice gave rise to undifferentiated sarcomas that expressed PDGFR-β, albeit with a reduced efficiency and increased latency compared to that observed by Sato and colleagues. These differences may reflect differences in the efficiency of recombination in the *Pdgfrb-Cre* and *Ng2/Cspg4-Cre* mice or may be due to distinct pericyte subpopulations that are marked by PDGFR-β and NG2 during development [42]. In the future, use of a conditional *Pdgfrb-iCreER*^{T2} mouse [43] that allows specific deletion of *Trp53* in the adult where *Pdgfrb* expression is restricted to pericytes, will allow further evaluation of the role of distinct mesenchymal cell lineages to the development of different sarcoma sub-types.

To address whether direct targeting of adult endothelial cells would result in the development of angiosarcomas with higher efficiency we used the *Cdh5-CreER*^{T2} mouse. Surprisingly all *Cdh5-CreER*^{T2}*, Trp53*$^{R172H/R172H}$ mice developed lymphomas. Studies in *Cdh5-CreER*^{T2} mice have reported recombination of a small (0.3%) subpopulation of bone marrow cells that are hematopoietic in nature [44]. Combined with the propensity of mutant p53 to drive lymphomagenesis this appears sufficient to drive development of lymphomas in the *Cdh5-*

CreER^{T2}, *Trp53*$^{R172H/R172H}$ mice. However, all of the *Cdh5-CreER*^{T2}, *Trp53*$^{fl/fl}$ mice developed angiosarcomas with no lymphomas detected. The enrichment of genes associated with p53 in the differentially expressed genes between the tumours that develop in the two models indicates that, as expected, the gain of function *Trp53R172H* mutant drives expression of a different set of genes to those seen in the *Cdh5-CreER*^{T2}, *Trp53*$^{fl/fl}$ mice, to initiate angiosarcoma development. Other mouse models targeting specific endothelial cell populations have also been reported. mTORC1 activation in endothelial cells following conditional deletion of its upstream inhibitor *Tsc1* resulted in 100% of mice developing hepatic hemangiomas, and around 80% developing cutaneous lymphangiosarcomas [45]. This is in contrast to the aggressive angiosarcomas that developed upon direct targeting of *Trp53* in endothelial cell lineages in the *Cdh5-CreER*^{T2}, *Trp53*$^{fl/fl}$ mice. mTORC1 pathway activation has also been reported in human angiosarcomas [45,46] and has been linked to Myc-mediated transcriptional regulation of VEGF [45]; increased expression of both *Myc* and *Vegfa* in the angiosarcomas from the *Cdh5-CreER*^{T2}, *Trp53*$^{fl/fl}$ mice suggest that a similar autocrine stimulation loop may be present in these tumours, although the involvement of mTORC signaling in these tumours is not known. Combined loss of *Trp53*, *Pten* and *Ptpn12* also leads to the development of aggressive vascular lesions which was associated with both mTORC and MEK pathway activation suggesting that mTORC activation alone is not sufficient to drive aggressive angiosarcoma development [46]. In this study loss of *Trp53* alone did not result in the development of angiosarcomas. However, the tumours arose from more restricted recombination in a sub-set of endothelial cells. Taken together with the distinctive spectrum of tumours seen upon deletion of *Tsc1* this suggests that targeting distinct populations of endothelial cells in mice in combination with differential pathway activation impacts on the type and site of vascular tumour development.

Increased Myc expression downstream of the forkhead boxO (FoxO) pathway has been linked to endothelial cell proliferation and angiosarcoma development [48,49]. Interestingly, conditional triple knock-out of FOXO1, 3, 4 in mice results in development of thymic lymphomas and vascular lesions, predominantly haemangiomas, in a number of tissues with only 9% progressing to angiosarcomas, although there is no reported role for Myc in this model [38]. This is in contrast to the *Cdh5-CreER*^{T2}, *Trp53*$^{fl/fl}$ mice where angiosarcomas arise predominantly in soft tissues as the vascular lesions that develop in the FOXO triple knock out mice are predominantly benign and arise in relation to the uterus and a number of other tissues [38]. FOXOs and p53 share many common target genes and may act in a cooperative manner in order to regulate gene transcription [50,51]. It will be interesting to establish whether the deregulation of such pathways is required for driving the transition from benign to malignant disease in the mouse models.

Angiosarcomas in humans may be divided into several clinical groups. The majority of cases, around 50%, are cutaneous, breast parenchymal angiosarcomas account for around 14% of angiosarcomas, soft tissue 11%, heart 7% and bone 4% with a range of other sites accounting for the remainder [47]. Little is known of the factors that predispose to angiosarcoma development in the clinical setting and it may be that angiosarcomas constitute a range of interrelated clinical diseases with common endothelial features but different phenotypes and aetiologies. Comparison of gene expression profiles between the two mouse models and human angiosarcomas showed significant enrichment of angiosarcoma associated genes in the two models suggesting that the mouse models do represent some of the phenotypes present in the human disease. Use of these and other mouse models will help to unravel some of the targetable pathways in angiosarcoma.

Although genetically engineered models are used in preclinical studies, the long latency of tumour formation in the *Cdh5-CreER*^{T2}, *Trp53*$^{fl/fl}$ mice (median lifespan 325 days) and the development of multiple tumours, would make therapeutic efficacy studies costly and challenging. Knock-out of p53 in alymphocytic Rag2−/−;Il2rg−/− mice leads to a high frequency of angiosarcomas (over 65%) with only sporadic formation of lymphomas. With a mean latency of 18 weeks this provides an alternative model that would be more amenable to therapeutic studies [12]. However, the lack of immune cell populations in these mice restricts their use for assessing immune modulators which are showing promise in sarcoma. A recent report has shown that use of a lentiviral vector-based system to introduce oncogenic *Hras*^{G12V} in combination with loss of *Cdkn2a* via intravenous injection into immune competent mice resulted in the formation of angiosarcomas. These develop very rapidly and in multiple sites which is most likely influenced by the intravenous route of injection [40]. This provides a useful model for preclinical studies but the rapid development of multiple tumours will make these studies challenging.

To overcome these issues, we generated cell lines from angiosarcomas that developed in the *Pdgfrb-Cre*, *Trp53*$^{R172H/R172H}$ and *Cdh5-CreER*^{T2}, *Trp53*$^{fl/fl}$ mice in an attempt to generate syngeneic mouse models of angiosarcoma. However, as has been reported previously [11], endothelial makers were rapidly lost when the tumours were established in culture, even when grown with endothelial cell specific supplements. In contrast, direct implantation of tumour fragments allowed us to establish angiosarcomas which could be frozen and passaged serially through wild type recipient mice. This had the benefit of reducing the latency of tumour formation while also restricting the number of tumours per mouse. Furthermore, the sub-

cutaneous localization of the tumours allowed easy monitoring of tumour growth. We have used this transplantation approach previously to model HER2 breast cancer and have demonstrated its utility in determining drug efficacy and establishing models of drug resistance [34].

Taken together our data indicate that deleting p53 in endothelial cells in the adult mouse is the most effective way to generate angiosarcomas. This resulted in 100% penetrance with no formation of lymphomas. The development of lymphomas in the *Cdh5-CreER*^{T2}, *Trp53*$^{R172H/R172H}$ mice supports a strong selection for angiosarcoma formation following loss of p53 in contrast to expression of the gain-of-function mutant p53. This is supported by angiosarcoma formation in mice in which loss of *Trp53* is combined with loss of *Ptpn12* and *Pten* [41]. The further establishment of a transplantation model of angiosarcoma provides a novel approach for testing potential new therapeutics in this disease setting.

Acknowledgements

This work was supported by Cancer Research UK grants (C157/A15703, C157/A9148 and C6088/A12063), a Wellcome Trust Senior Research Fellowship in Clinical Science 103749) to N.C.H., a Wellcome Trust Clinical Training Fellowship to J.R.S, a Wellcome Trust Institutional Strategic Support Fund award, the Edinburgh and Lothian Health Foundation Margaret Lee Oncology fund, the Charon Fund and NHS Research Scotland.

Author contributions

H.C., M.M., K.T., J.C., J.C.S. M.G., K.M., A.H.S. and L.G.C. carried out the experiments and analyzed the data. D.M.S. carried out the histological evaluation. N.C.H., D.M.S., L.H. and V.G.B. conceived and designed the experiments and D.M.S. and V.G.B. wrote the manuscript.

References

1. Young RJ, Brown NJ, Reed MW, *et al.* Angiosarcoma. *Lancet Oncol* 2010; **11**: 983-991.
2. Behjati S, Tarpey PS, Sheldon H, *et al.* Recurrent PTPRB and PLCG1 mutations in angiosarcoma. *Nat Genet* 2014; **46**: 376-379.
3. Hung J, Hiniker SM, Lucas DR, *et al.* Sporadic versus Radiation-Associated Angiosarcoma: A Comparative Clinicopathologic and Molecular Analysis of 48 Cases. *Sarcoma* 2013; **2013**: 798403.
4. Italiano A, Chen CL, Thomas R, *et al.* Alterations of the p53 and PIK3CA/AKT/mTOR pathways in angiosarcomas: a pattern distinct from other sarcomas with complex genomics. *Cancer* 2012; **118**: 5878-5887.
5. Murali R, Chandramohan R, Moller I, *et al.* Targeted massively parallel sequencing of angiosarcomas reveals frequent activation of the mitogen activated protein kinase pathway. *Oncotarget* 2015; **6**: 36041-36052.
6. Naka N, Tomita Y, Nakanishi H, *et al.* Mutations of p53 tumor-suppressor gene in angiosarcoma. *Int J Cancer* 1997; **71**: 952-955.
7. Weihrauch M, Markwarth A, Lehnert G, *et al.* Abnormalities of the ARF-p53 pathway in primary angiosarcomas of the liver. *Human Pathol* 2002; **33**: 884-892.
8. Zietz C, Rossle M, Haas C, *et al.* MDM-2 oncoprotein overexpression, p53 gene mutation, and VEGF up-regulation in angiosarcomas. *Am J Pathol* 1998; **153**: 1425-1433.
9. Donehower LA, Harvey M, Slagle BL, *et al.* Mice deficient for p53 are developmentally normal but susceptible to spontaneous tumours. *Nature* 1992; **356**: 215-221.
10. Jacks T, Remington L, Williams BO, *et al.* Tumor spectrum analysis in p53-mutant mice. *Curr Biol* 1994; **4**: 1-7.
11. Farhang Ghahremani M, Radaelli E, Haigh K, *et al.* Loss of autocrine endothelial-derived VEGF significantly reduces hemangiosarcoma development in conditional p53-deficient mice. *Cell Cycle* 2014; **13**: 1501-1507.
12. Landuzzi L, Ianzano ML, Nicoletti G, *et al.* Genetic prevention of lymphoma in p53 knockout mice allows the early development of p53-related sarcomas. *Oncotarget* 2014; **5**: 11924-11938.
13. Charytonowicz E, Cordon-Cardo C, Matushansky I, *et al.* Alveolar rhabdomyosarcoma: is the cell of origin a mesenchymal stem cell? *Cancer Lett* 2009; **279**: 126-136.
14. Matushansky I, Hernando E, Socci ND, *et al.* Derivation of sarcomas from mesenchymal stem cells via inactivation of the Wnt pathway. *J Clin Invest* 2007; **117**: 3248-3257.
15. Riggi N, Cironi L, Provero P, *et al.* Development of Ewing's sarcoma from primary bone marrow-derived mesenchymal progenitor cells. *Cancer Res* 2005; **65**: 11459-11468.
16. Rubio R, Garcia-Castro J, Gutierrez-Aranda I, *et al.* Deficiency in p53 but not retinoblastoma induces the transformation of mesenchymal stem cells in vitro and initiates leiomyosarcoma in vivo. *Cancer Res* 2010; **70**: 4185-4194.
17. Sato S, Tang YJ, Wei Q, *et al.* Mesenchymal Tumors Can Derive from Ng2/Cspg4-Expressing Pericytes with beta-Catenin Modulating the Neoplastic Phenotype. *Cell Rep* 2016; **16**: 917-927.
18. Tirode F, Laud-Duval K, Prieur A, *et al.* Mesenchymal stem cell features of Ewing tumors. *Cancer Cell* 2007; **11**: 421-429.

19. Caplan AI. All MSCs are pericytes? *Cell stem cell* 2008; **3**: 229-230.
20. Crisan M, Yap S, Casteilla L, *et al.* A perivascular origin for mesenchymal stem cells in multiple human organs. *Cell Stem Cell* 2008; **3**: 301-313.
21. Benassi MS, Pazzaglia L, Chiechi A, *et al.* NG2 expression predicts the metastasis formation in soft-tissue sarcoma patients. *J Orthop Res* 2009; **27**: 135-140.
22. Wei Q, Tang YJ, Voisin V, *et al.* Identification of CD146 as a marker enriched for tumor-propagating capacity reveals targetable pathways in primary human sarcoma. *Oncotarget* 2015; **6**: 40283-40294.
23. Foo SS, Turner CJ, Adams S, *et al.* Ephrin-B2 controls cell motility and adhesion during blood-vessel-wall assembly. *Cell* 2006; **124**: 161-173.
24. Henderson NC, Arnold TD, Katamura Y, *et al.* Targeting of alphav integrin identifies a core molecular pathway that regulates fibrosis in several organs. *Nat Med* 2013; **19**: 1617-1624.
25. Stanczuk L, Martinez-Corral I, Ulvmar MH, *et al.* cKit Lineage Hemogenic Endothelium-Derived Cells Contribute to Mesenteric Lymphatic Vessels. *Cell Rep* 2015.
26. Ulvmar MH, Martinez-Corral I, Stanczuk L, *et al.* Pdgfrb-Cre targets lymphatic endothelial cells of both venous and non-venous origins. *Genesis* 2016; **54**: 350-358.
27. Wang Y, Nakayama M, Pitulescu ME, *et al.* Ephrin-B2 controls VEGF-induced angiogenesis and lymphangiogenesis. *Nature* 2010; **465**: 483-486.
28. Blagosklonny MV. p53 from complexity to simplicity: mutant p53 stabilization, gain-of-function, and dominant-negative effect. *FASEB J* 2000; **14**: 1901-1907.
29. Sigal A, Rotter V. Oncogenic mutations of the p53 tumor suppressor: the demons of the guardian of the genome. *Cancer Res* 2000; **60**: 6788-6793.
30. Lang GA, Iwakuma T, Suh YA, *et al.* Gain of function of a p53 hot spot mutation in a mouse model of Li-Fraumeni syndrome. *Cell* 2004; **119**: 861-872.
31. Olive KP, Tuveson DA, Ruhe ZC, *et al.* Mutant p53 gain of function in two mouse models of Li-Fraumeni syndrome. *Cell* 2004; **119**: 847-860.
32. Jonkers J, Meuwissen R, van der Gulden H, *et al.* Synergistic tumor suppressor activity of BRCA2 and p53 in a conditional mouse model for breast cancer. *Nat Genet* 2001; **29**: 418-425.
33. Madisen L, Zwingman TA, Sunkin SM, *et al.* A robust and high-throughput Cre reporting and characterization system for the whole mouse brain. *Nat Neurosci* 2010; **13**: 133-140.
34. Creedon H, Balderstone LA, Muir M, *et al.* Use of a genetically engineered mouse model as a preclinical tool for HER2 breast cancer. *Dis Model Mech* 2016; **9**: 131-140.
35. Lynch RW, Hawley CA, Pellicoro A, *et al.* An efficient method to isolate Kupffer cells eliminating endothelial cell contamination and selective bias. *J Leukoc Biol* 2018; **104**: 579-586.
36. Eisen MB, Spellman PT, Brown PO, *et al.* Cluster analysis and display of genome-wide expression patterns. *Proc Natl Acad Sci U S A* 1998; **95**: 14863-14868.
37. Subramanian A, Tamayo P, Mootha VK, *et al.* Gene set enrichment analysis: a knowledge-based approach for interpreting genome-wide expression profiles. *Proc Natl Acad Sci U S A* 2005; **102**: 15545-15550.
38. Paik JH, Kollipara R, Chu G, *et al.* FoxOs are lineage-restricted redundant tumor suppressors and regulate endothelial cell homeostasis. *Cell* 2007; **128**: 309-323.
39. Andersen NJ, Nickoloff BJ, Dykema KJ, *et al.* Pharmacologic inhibition of MEK signaling prevents growth of canine hemangiosarcoma. *Mol Cancer Ther* 2013; **12**: 1701-1714.

40. Yang J, Ren Z, Du X, *et al.* The role of mesenchymal stem/progenitor cells in sarcoma: update and dispute. *Stem Cell Investig* 2014; **1**: 18.
41. Sa da Bandeira D, Casamitjana J, Crisan M. Pericytes, integral components of adult hematopoietic stem cell niches. *Pharmacol Ther* 2017; **171**: 104-113.
42. Birbrair A, Zhang T, Wang ZM, *et al.* Role of pericytes in skeletal muscle regeneration and fat accumulation. *Stem Cells Dev* 2013; **22**: 2298-2314.
43. Claxton S, Kostourou V, Jadeja S, *et al.* Efficient, inducible Cre-recombinase activation in vascular endothelium. *Genesis* 2008; **46**: 74-80.
44. Monvoisin A, Alva JA, Hofmann JJ, *et al.* VE-cadherin-CreERT2 transgenic mouse: a model for inducible recombination in the endothelium. *Dev Dyn* 2006; **235**: 3413-3422.
45. Sun S, Chen S, Liu F, *et al.* Constitutive Activation of mTORC1 in Endothelial Cells Leads to the Development and Progression of Lymphangiosarcoma through VEGF Autocrine Signaling. *Cancer Cell* 2015; **28**: 758-772.
46. Chadwick ML, Lane A, Thomas D, *et al.* Combined mTOR and MEK inhibition is an effective therapy in a novel mouse model for angiosarcoma. *Oncotarget* 2018; **9**: 24750-24765.
47. Lahat G, Dhuka AR, Hallevi H, *et al.* Angiosarcoma: clinical and molecular insights. *Ann Surg* 2010; **251**: 1098-1106.
48. Riddell M, Nakayama A, Hikita T, *et al.* aPKC controls endothelial growth by modulating c-Myc via FoxO1 DNA-binding ability. *Nat Commun* 2018; **9**: 5357.
49. Wilhelm K, Happel K, Eelen G, *et al.* FOXO1 couples metabolic activity and growth state in the vascular endothelium. *Nature* 2016; **529**: 216-220.
50. Fu Z, Tindall DJ. FOXOs, cancer and regulation of apoptosis. *Oncogene* 2008; **27**: 2312-2319.
51. Renault VM, Thekkat PU, Hoang KL, *et al.* The pro-longevity gene FoxO3 is a direct target of the p53 tumor suppressor. *Oncogene* 2011; **30**: 3207-3221.
52. Derksen PW, Liu X, Saridin F, *et al.* Somatic inactivation of E-cadherin and p53 in mice leads to metastatic lobular mammary carcinoma through induction of anoikis resistance and angiogenesis. *Cancer Cell* 2006; **10**: 437-449.

Figures

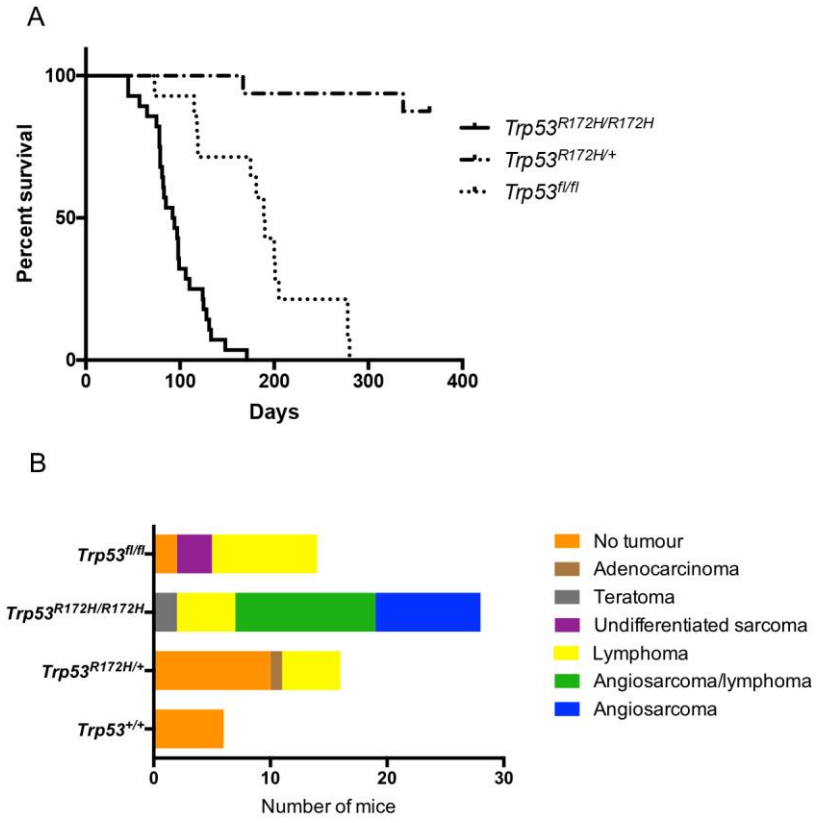

Figure 1. Tumour development in *Pdgfrb-Cre* mice. (A) Kaplan-Meier curves showing significant difference in survival between *Trp53*$^{R172H/R172H}$ (n=28), *Trp53*$^{R172H/+}$ (n=16) and Trp53$^{fl/fl}$ (n=14) mice (log-rank $p < 0.0001$). (B) Tumour incidence and type in the different mouse cohorts.

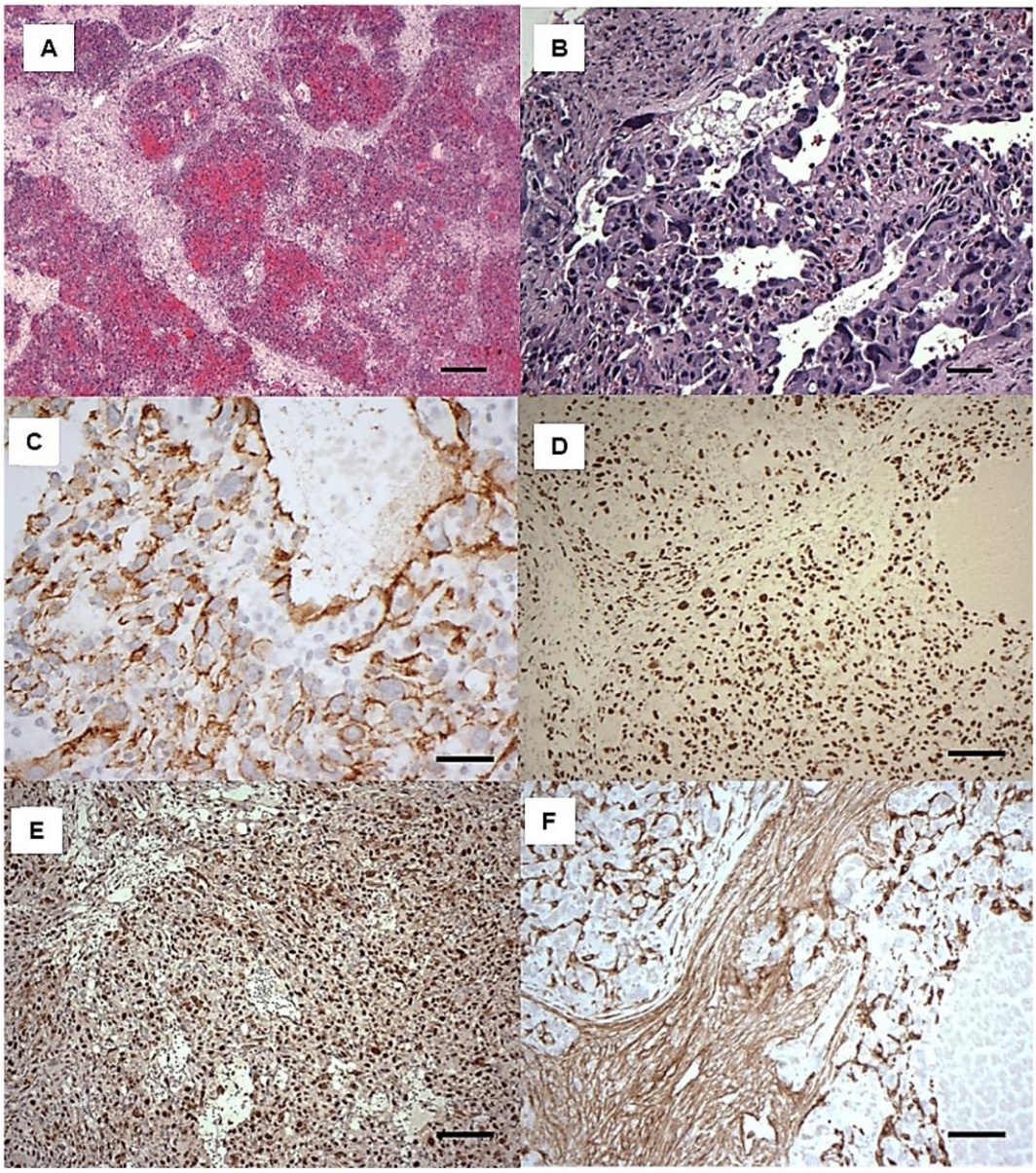

Figure 2. Histology and immunohistochemistry of mouse angiosarcomas in *Pdgfrb-Cre*, *Trp53*$^{R172H/R172H}$ mice. (A, B) H&E staining showed vascular, lobulated tumour masses: scale bar = 500 μm. These were composed of pleomorphic tumour cells showing variable vasoformative capability: scale bar = 50 μm (B). (C-F) Immunohistochemical analysis with antibodies to (C) CD31: scale bar = 50 μm; (D) ERG: scale bar = 250 μm; (E) p53: scale bar = 250 μm and (F) PDGFR-β: scale bar = 50 μm.

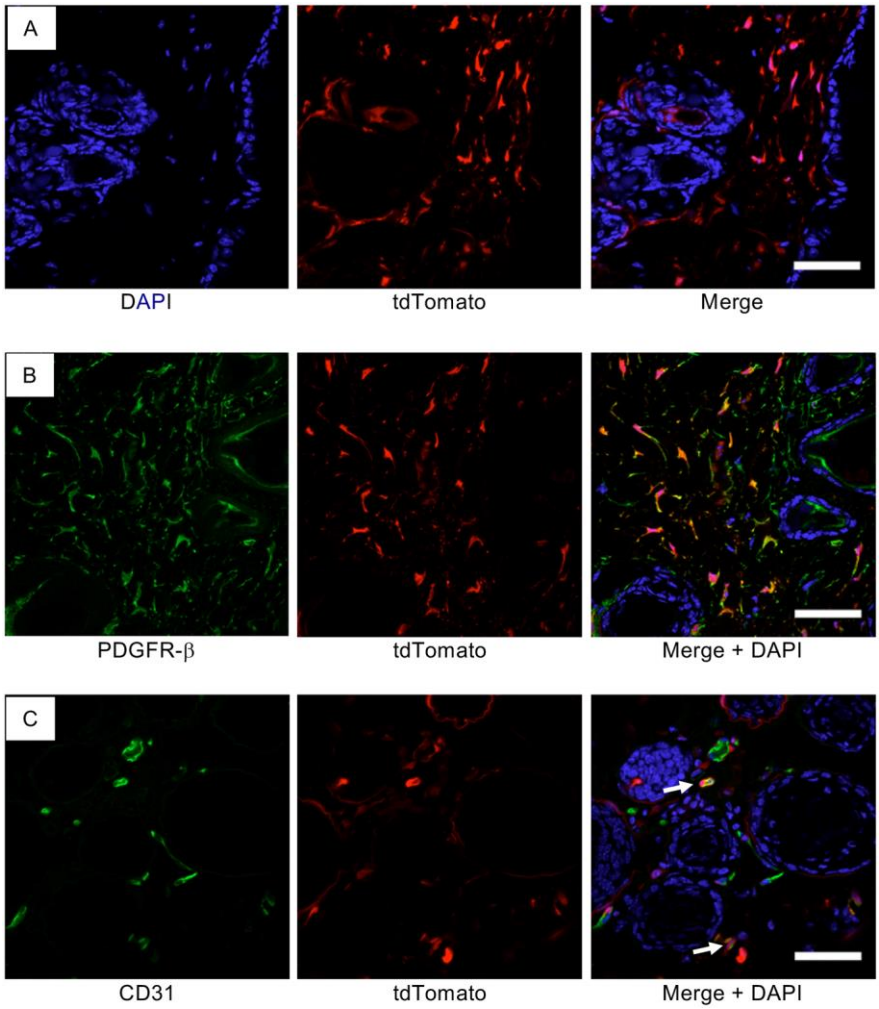

Figure 3. PDGFRβ does not co-localize with CD31 in mouse skin. Confocal micrographs of fixed frozen dorsal skin from the *Pdgfrb-Cre* mouse crossed with a tdTomato floxed reporter (*Ai14;Pdgfrb-Cre*) showing (A) tdTomato fluorescence (red) (B) PDGFRβ antibody staining (green) and (C) CD31 antibody staining (green). DAPI (blue) indicates nuclei. Arrow demonstrates a CD31 labeled endothelial cell surrounded by a tdTomato positive perivascular cell: scale bars = 50 μm.

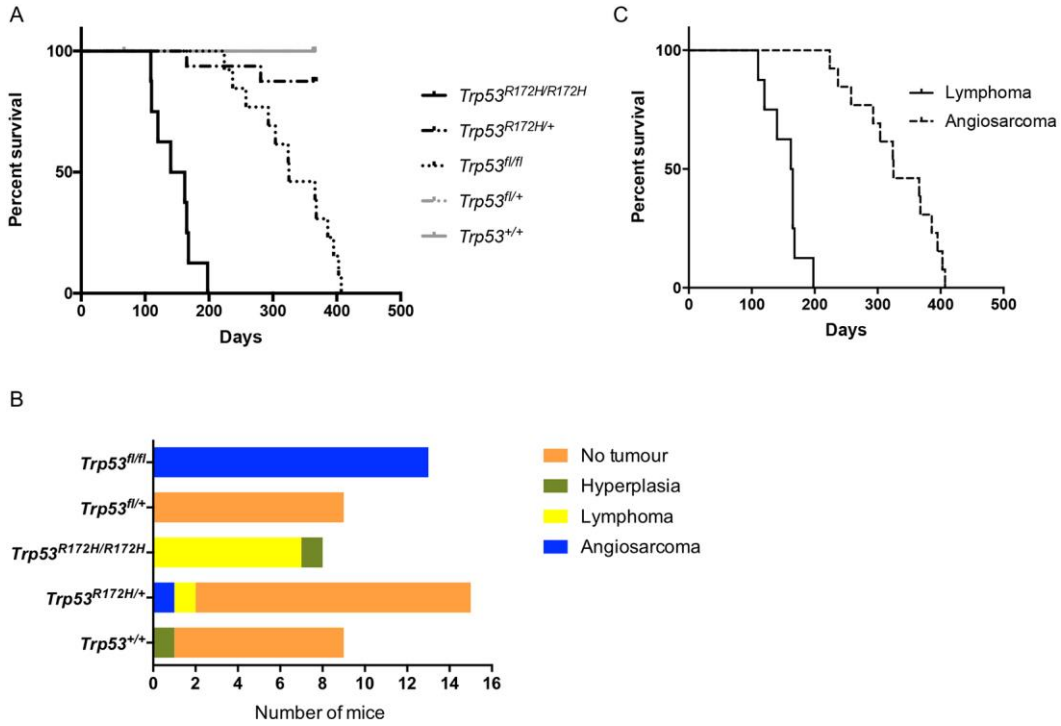

Figure 4. Tumour development in *Cdh5-CreER*^{T2} mice. **(**A) Kaplan-Meier curves showing significant difference in survival between different mouse cohorts (log-rank $p < 0.0001$). (B) Tumour incidence and type in the different mouse cohorts. (C) Kaplan-Meier curves showing significant difference in survival between mice developing angiosarcomas and lymphomas (log-rank $p < 0.0001$).

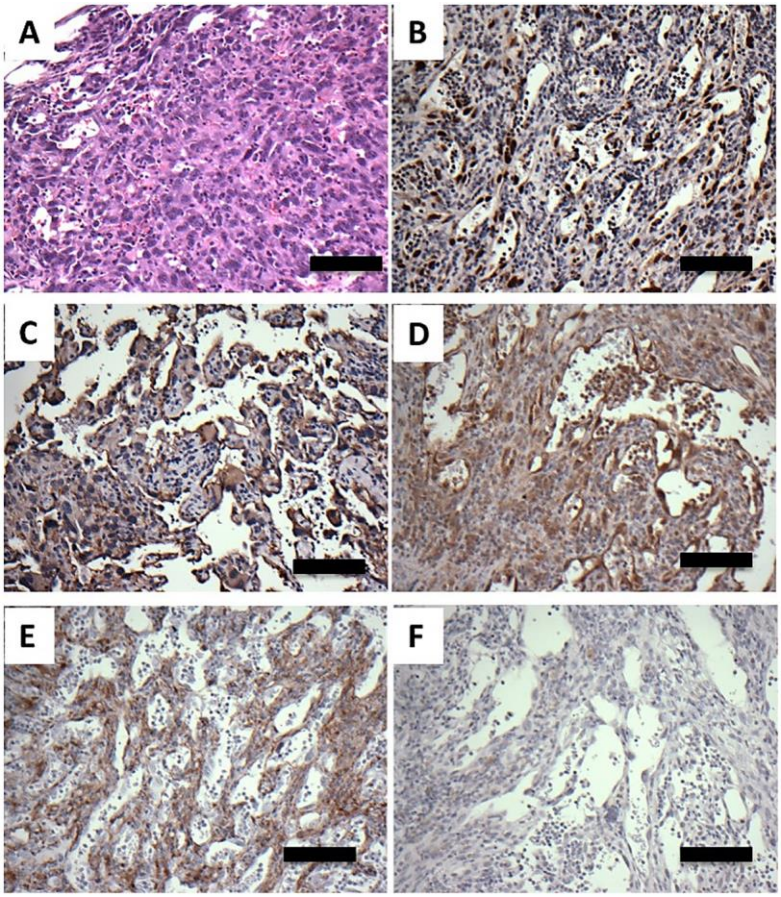

Figure 5. Histology of and immunohistochemistry of mouse angiosarcomas in *Cdh5-CreER*^{T2}, *Trp53*$^{fl/fl}$ mice. (A) H&E staining showing atypical cells lining vascular channels: scale bar = 50 μm. (B–F) Immunohistochemical analysis using antibodies to (B) ERG; (C) CD31 and (D) VE-cadherin, (E) PDGFRβ and (F) p53. Scale bars = 100 μm.

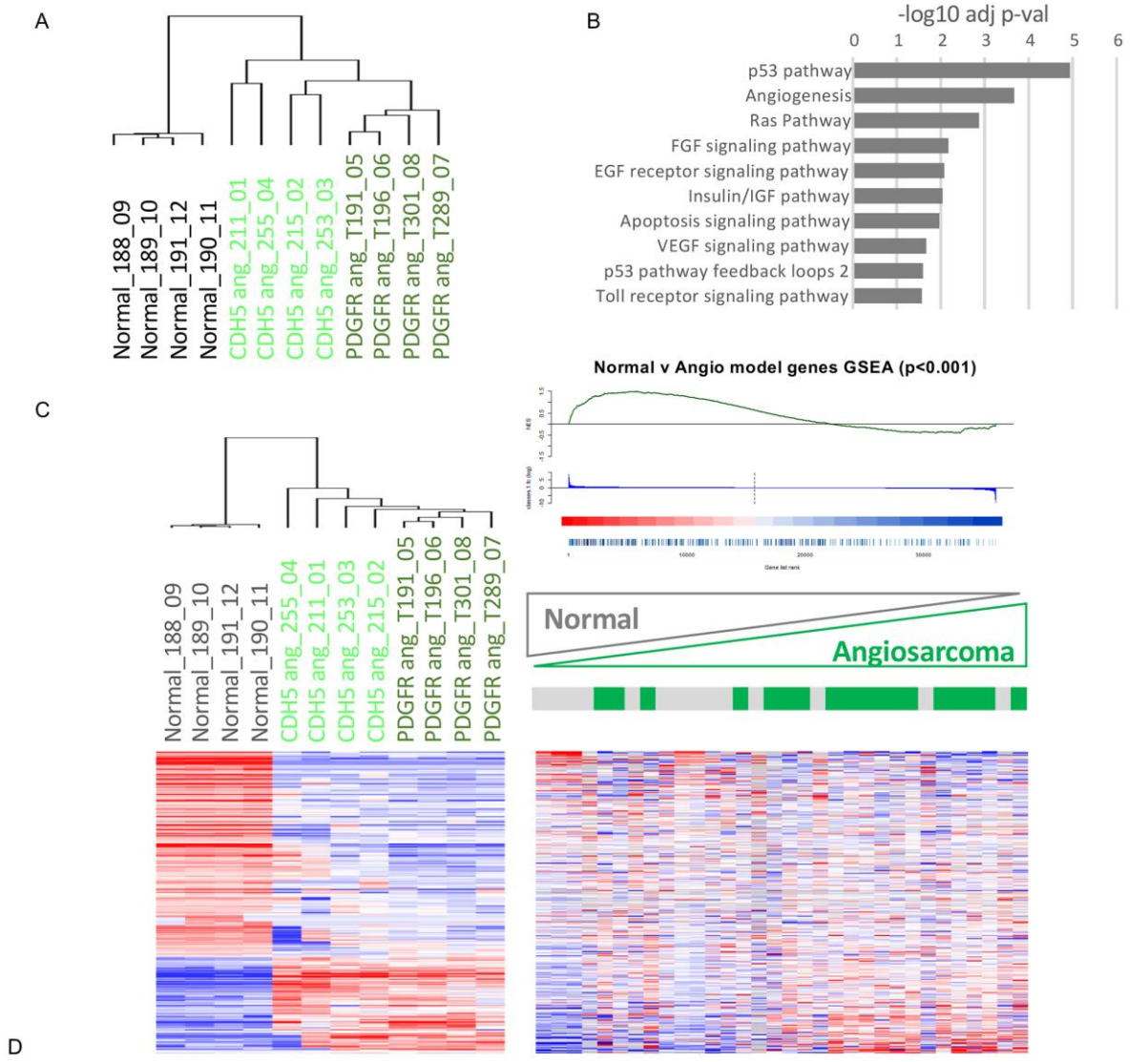

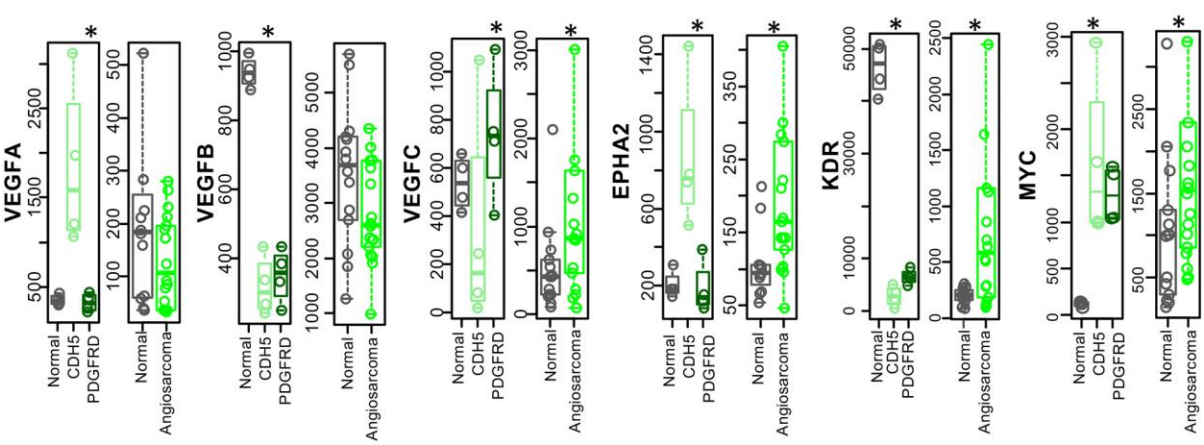

Figure 6. Gene expression analysis demonstrates mouse angiosarcomas have common and distinct features, but largely resemble human angiosarcomas. (A) Unsupervised hierarchical clustering of the NanoString PanCancer Pathways panel demonstrated some variation between the mouse angiosarcomas, but are significantly more different than normal Cdh5 derived endothelial cells. (B) Analysis of PANTHER signalling pathways that were significantly differentially expressed between the two mouse angiosarcomas. (C) The 299 significantly differently expressed genes between the mouse angiosarcomas and normal Cdh5 derived endothelial cells were significantly enriched in human angiosarcomas compared to normal human endothelial cells. (D) Genes associated with endothelial cell function were significantly increased in angiosarcomas in both the human and mouse datasets (VEGFC, EPHA2), while others were significantly (*$p<0.05$, Wilcoxon rank-sum test) differentially regulated in the human and mouse angiosarcomas (VEGF, VEGFB, KDR and MYC).

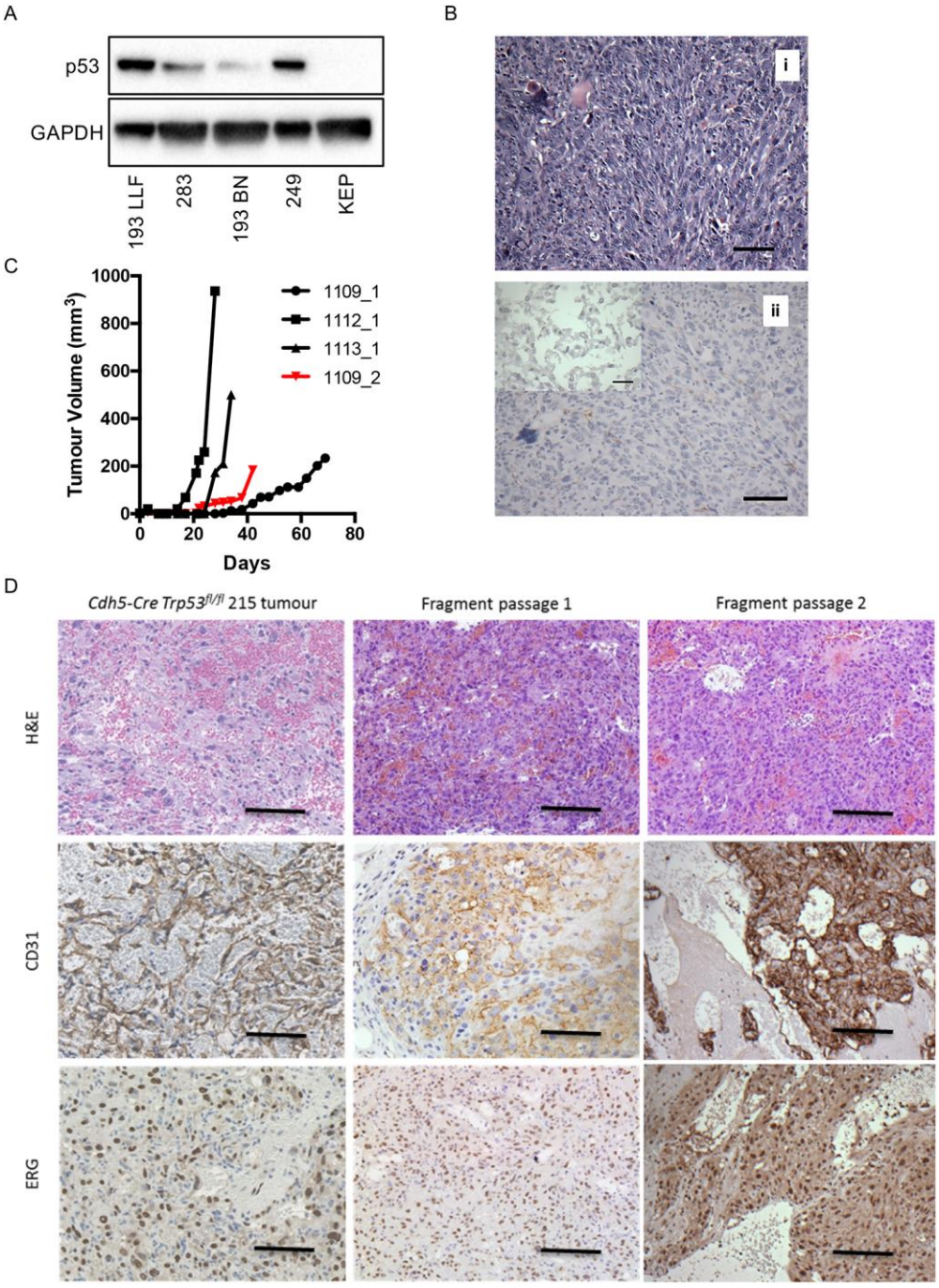

Figure 7. Characterization of cell lines and fragment-derived tumours from mouse angiosarcomas. (A) Western blot analysis of p53 expression in 4 *Pdgfrb-Cre*, *Trp53*$^{R172H/R172H}$ angiosarcoma derived cell lines. KEP are a mouse mammary tumour cell line that is deficient in p53 due to homozygous expression of a floxed p53 allele [52]. GAPDH was used as a loading control. (B) The morphology of tumours developing following implantation of

angiosarcoma derived cell lines was that of undifferentiated pleomorphic sarcomas (i) H&E, scale bar = 50 μm. ii) Immunohistochemical analysis using antibody to CD31. The tumour cells were negative for CD31 as was the implanted angiosarcoma derived cell line (inset). Scale bar = 50 μm; inset 25 μm. (C) Growth of tumour fragments taken from 3 different *Cdh5-CreER*^{T2}, *Trp53*$^{fl/fl}$ mice following sub-cutaneous transplantation into wild type mice. 1109_2 is the secondary transplantation of fragments derived from tumour 1109_1. (D) H&E staining and immunohistochemistry of *Cdh5-CreER*^{T2}, *Trp53*$^{fl/fl}$ fragment-derived tumours. Left hand panels spontaneous tumour, middle panel primary passage of tumour fragments, right hand panels secondary passage of tumour fragments. Scale bar = 50 μm

Table 1: Incidence of angiosarcoma formation in *Pdgfrb*-Cre, $p53^{R172H/R172H}$ mice

Mouse ID	Number	Position
24	3	Hip, shoulder, leg
152	5	Abdomen, flank, knee, hip, shoulder,
156	2	Mammary fat pad, leg
187	3	Heart, intramuscular back, fat shoulder
191	5	Shoulder, flank, mammary fat pad, abdomen, back
193	4	Back, neck, flank, abdomen
194	1	Mammary fat pad
195	3	Heart, intramuscular leg, armpit
196	3	Shoulder, back, neck
197	1	Flank
215	6	Shoulder, intramuscular abdomen, sub-cutaneous back (x2), preputial, peritoneum
249	2	Sub-cutaneous back, soft tissue chest
251	2	Muzzle, leg
259	2	Leg, diaphragm.
265	3	Diaphragm, heart, sub-cutaneous back
283	2	Shoulder, mammary fat pad
289	2	Leg, chest
291	6	Leg, mid abdomen, lower abdomen, back, neck, mammary fat pad
298	2	Mammary fat pad (x2)
301	3	Peritoneum, chest, shoulder
330	2	Stomach, heart

Table 2: Incidence of angiosarcoma formation in *Cdh5*-Cre, $p53^{fl/fl}$ mice

Mouse ID	**Number**	**Position**
181	5	Mediastinal, intrabdominal, genital
208	1	Shoulder
210	1	Intrabdominal
211	2	Hip, intrabdominal
214	2	Intrabdominal, mammary fat pad
215	1	Mediastinal, intrabdominal, perirenal
216	3	Genital, perirenal, mammary fat pad
247	3	Intrabdominal, genital
253	1	Genital
254	6	Mediastinal, intrabdominal, mammary fat pad
255	1	Shoulder

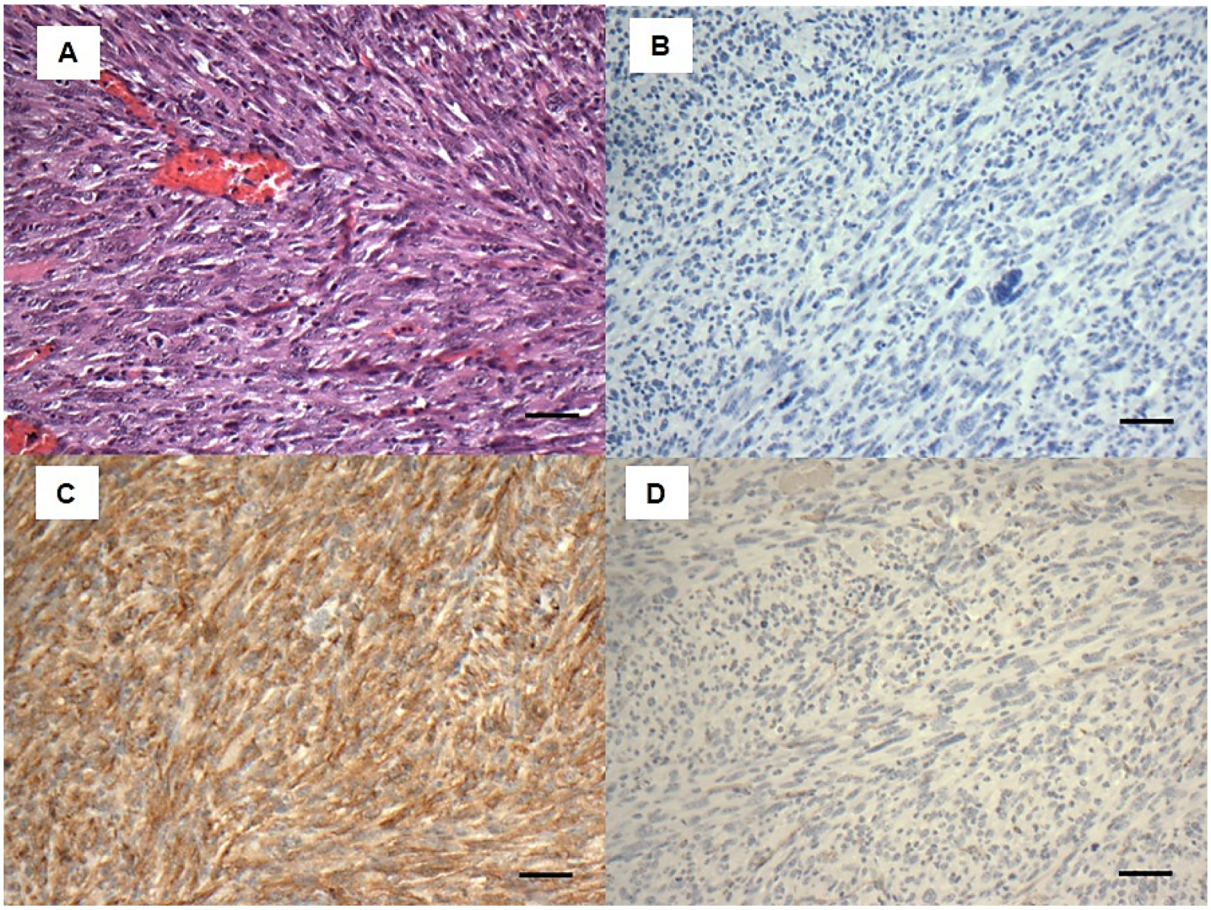

Figure S1. Immunohistochemistry of mouse undifferentiated sarcomas. (A) H&E staining showed tumours comprising spindle and pleomorphic cells without evidence of specific lineage differentiation histologically. Cells were (B) negative for p53, (C) positive for PDGRFβ and (D) negative for CD31. Scale bars = 50 μm.

A

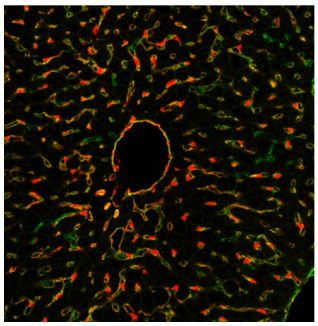

B

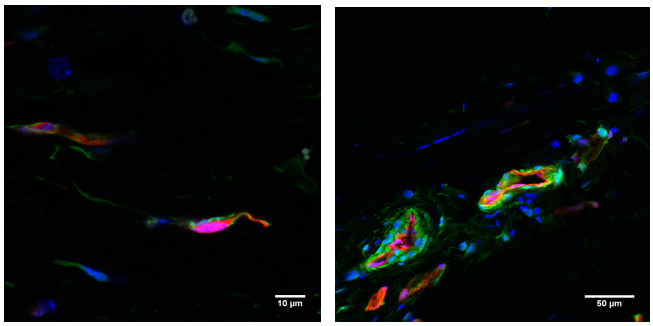

Figure S2. Confocal micrographs of fixed frozen liver (A) and dorsal skin (B) from *Cdh5-CreER*^{T2} mouse crossed with a tdTomato floxed reporter (*Ai14; Cdh5-CreER*^{T2}) showing cytosolic tdTomato fluorescence (red) and CD31 antibody cell surface staining (green). DAPI (blue) indicates nuclei.